Decoupling peroxyacetyl nitrate from ozone in Chinese outflows observed at Gosan Climate Observatory

Jihyun Han[1*], Meehye Lee[1], Gangwoong Lee[2], Louisa K. Emmons[3]

[1]Department of Earth and Environmental Sciences, Korea University, Seoul, Republic of Korea

[2]Department of Environmental Science, Hankuk University of Foreign Studies, Yongin, Republic of Korea

[3]Atmospheric Chemistry Observations and Modeling Laboratory, National Center for Atmospheric Research (NCAR), Boulder, CO, USA

*now at: Korea Environment Institute, Sejong, Republic of Korea

Correspondence to: M. Lee (meehye@korea.ac.kr)

Submitted to Atmospheric Chemistry and Physics

December 2016

Abstract

We measured peroxyacetyl nitrate (PAN) and other reactive species such as O_3, NO_2, CO, and SO_2 with aerosols including mass, organic carbon (OC), and elemental carbon (EC) in $PM_{2.5}$ and K^+ in $PM_{1.0}$ at Gosan Climate Observatory in Korea (33.17°N, 126.10°E) during October 10 to November 6, 2010. PAN was determined through fast gas chromatography with luminol chemiluminescence detection at 425 nm every 2 min. The PAN concentrations ranged from 0.1 (detection limit) to 2.4 ppbv with a mean of 0.6 ppbv. For all measurements, PAN was unusually better correlated with $PM_{2.5}$ (Pearson correlation coefficient, $\gamma = 0.79$) than with O_3 ($\gamma = 0.67$). In particular, the O_3 level was highly elevated with SO_2 at midnight, along with a typical midday peak when air was transported rapidly from the Beijing areas. The PAN enhancement was most noticeable during the occurrence of haze under stagnant conditions. In Chinese outflows slowly transported over the Yellow Sea, PAN gradually increased up to 2.4 ppbv at night, in excellent correlation with a concentration increase of $PM_{2.5}$ OC and EC, $PM_{2.5}$ mass, and $PM_{1.0}$ K^+. The high K^+ concentration and OC/EC ratio indicated that the air mass was impacted by biomass combustion. This study highlights PAN decoupling with O_3 in Chinese outflows and suggests PAN as a useful indicator for diagnosing continental outflows and assessing their perturbation on regional air quality in northeast Asia.

Key words: PAN, O_3, $PM_{2.5}$, Chinese outflow, Haze, Biomass combustion

1. Introduction

At the surface, ozone is primarily photochemically produced, and the contribution from the stratosphere is generally small. Ozone is formed through reactions of various precursors such as CO, CH_4, volatile organic compounds (VOCs), and NO_x (e.g., Brasseur et al., 1999; Jacob, 2000; Nielsen et al., 1981). Likewise, peroxyacetyl nitrate (PAN) is a secondary product of urban air pollution and a significant oxidant in the atmosphere (e.g., Hansel and Wisthaler, 2000; La Franchi et al., 2009; Lee et al., 2012; Liu et al., 2010; Roberts et al., 2007). PAN is solely produced by the photochemical reaction between the peroxyacetyl radical and nitrogen dioxide, and the peroxyacetyl radical is derived from the OH oxidation or photolysis of VOCs such as acetaldehyde, methylglyoxal, and acetone (e.g., Fischer et al., 2014; La Franchi et al., 2009; Lee et al., 2012). For this reason, PAN is a very useful indicator of photochemical air pollution. As thermal decomposition is a major PAN sink in the troposphere (Beine et al., 1997; Jacob, 2000; Kenley and Hendry, 1982; Talukdar et al., 1995), the lifetime of PAN depends on temperature. For example, the PAN lifetime is ~5 years at −26°C and 1 h at 20°C (Fischer et al., 2010; Zhang et al., 2011). At high altitudes above ~7 km, photolysis becomes the most important loss process for PAN (Talukdar, et al., 1995). Besides, PAN is less soluble compared to nitric acid and is more easily transported to the free troposphere after it is released from scavenge in lower temperature (e.g., Zhu et al., 2017). Thus, PAN can be an indicator of NO_y concentration in the free troposphere and a guide for the long-range transport of NO_x in remote regions (Jacob, 1999).

In the past decades, PAN was measured not only in urban areas (Aneja et al., 1999; Gaffney et al., 1999; Grosjean et al., 2002; Lee et al., 2008; Tanimoto et al., 1999; Zhang et al., 2014) but also in background regions (Fischer et al., 2011; Kanaya et al., 2007; Lee et al., 2012; Tanimoto et al., 2002), onboard aircraft (Tereszchuk et al., 2013), and ships (Roberts et

al., 2007). PAN concentrations were in the range of a few ppbv in urban areas close to VOCs and NO_x sources (Lee et al., 2008; Zhang et al., 2011). In the most remote regions, PAN concentrations were generally in the range of a few pptv (Gallagher et al., 1990; Mills et al., 2007; Muller and Rudolph, 1992; Staudt et al., 2003).

Although NO_x concentration has recently declined in China (Gu et al., 2013; Liu et al., 2016a; Krotkov et al., 2016), NO_x and VOCs have gradually increased in East Asia, particularly China during the last couple of decades (Akimoto, 2003; Liu et al., 2010; Ohara et al., 2007; Zhao et al., 2013). It led to an increase in the concentrations of photochemical byproducts such as PAN and O_3 not only in East Asia (Liu et al., 2010; Wang et al., 2010; Zhang et al., 2009; Zhang et al., 2011; Zhang et al., 2014) but also in North America (Fischer et al., 2010; Fischer et al., 2011; Jaffe et al., 2007; Zhang et al., 2008). These results were also demonstrated by the GEOS-Chem model (Zhang et al., 2008). In addition to urban plumes, PAN was reported to be enhanced by biomass combustion (Alvarado et al., 2010; Coheur et al., 2007; Zhu et al., 2015; Zhu et al., 2017), such as open burning and use of biofuel, which is used to take place often in China after crop harvesting (Cao et al., 2006; Duan et al., 2004). Recent satellite studies have also observed the increased PAN in plumes associated with anthropogenic emissions in eastern China and boreal fires in Siberia (Zhu et al., 2015; Zhu et al., 2017). In this context, PAN is a useful indicator for diagnosing Chinese outflows and assessing their perturbation on regional air quality in the northwestern Pacific region.

Gosan Climate Observatory (GCO) is an ideal place to monitor Asian outflows and their transformation and to estimate their impact on air quality over the northern Pacific region (Lee et al., 2007; Lim et al., 2012). In the present study, PAN was first measured continuously at GCO to characterize its variation and source in relation to O_3 and to

94 understand the influence of Chinese outflows on the regional air quality.

95

96 **2. Experiments**

97 PAN measurements were conducted at GCO (33.17°N, E126.10°E) on Jeju Island from
98 October 19 to November 6, 2010. GCO is located on a cliff at the western edge of Jeju Island.

99 PAN was determined through fast gas chromatography (GC) with luminol
100 chemiluminescence detection, which is described in detail elsewhere (Gaffney et al., 1998;
101 Lee et al., 2008; Marley et al., 2004). Here, we briefly describe the measurement method.

102 Ambient air was pumped through a 1.6-m PFA tubing (1/4 inch outer diameter) from the
103 roof of the two-story container into a six-port two-position switching injection valve
104 (Cheminert C22, Valco Instruments (Houston, TX, USA)) at 100 ml/min controlled by Mass
105 flow controller (Lee et al., 2012; Lee et al., 2008). The residence time of the inlet was less
106 than 2 seconds. PAN and NO_2 (and peroxypropyl nitrate (PPN) if present) were separated
107 along a 10-m capillary GC column (DB-1, J&W Scientific, Folsom, CA, USA), whose end
108 was connected to a luminol cell where the column effluent reacted with luminol, giving off
109 luminescent light (Lee et al., 2008; Lee et al., 2012). The concentrations of PAN and other
110 species were determined from the chemiluminescence signals detected by a gated photon
111 counter (HC135-01, Hamamatsu, Bridgewater, NJ, USA) at 425 nm, which was set at 800 V
112 and operated at room temperature (Gaffney et al., 1998; Lee et al., 2012; Lee et al., 2008).

113 PAN was calibrated against standards synthesized by the nitration of peracetic acid in n-
114 tridecane (Gaffney et al., 1984; Gregory, 1990; Lee et al., 2008). A few microliter aliquots of
115 standard solution were injected through an injection valve and then mixed with zero air
116 (99.999 %) in a 5 L Tedlar bag. After being left for a few minutes for equilibrium, it was
117 injected into GC-luminol instrument and NOx chemiluminescence instrument with a

molybdenum converter (42C, Thermo Electron Corporation, Franklin, MA, USA). The calibration was completed within 5 minutes to prevent thermal decomposition of the PAN (Kourtidis et al., 1993; Lee et al., 2008). These calibration procedures were carried out on the assumption that the PAN was completely converted to NO in the molybdenum converter. The detection limit of PAN defined by 3σ of the lowest standard was no greater than 100 pptv (Lee et al., 2008). The overall measurement uncertainty and precision was estimated to be 16 % and 5%, respectively (Lee et al., 2012). NO_x instrument was calibrated with NO standard gas.

Gaseous species including O_3, NO, NO_2, CO, and SO_2 were measured by UV absorption, chemiluminescence with a molybdenum converter, non-dispersive infrared, and pulse UV fluorescence method, respectively (NIER, 2016a). The measurements were made in compliance with guidelines for installation and operation of air pollution monitoring network (NIER, 2016b). Calibration was conducted before and after the experiment, following the regular checkup procedure. Detection limits of O_3, NO_x, CO, and SO_2 are 2 ppb, 0.1 ppb, 0.05 ppm, 0.1 ppb, respectively (NIER, 2016b).

Aerosol species, including $PM_{2.5}$ mass and $PM_{2.5}$ OC and EC were measured and recorded along with meteorological parameters (relative humidity, temperature, and wind speed). Water-soluble ions of $PM_{1.0}$ were collected by a particle-into-liquid sampler and analyzed by ion chromatography. The detailed results of the aerosol measurements can be found in Shang et al. (2017).

For the air parcel at 850 m a.s.l., the three-day backward trajectories were calculated every hour using NOAA Air Resources Laboratory (ARL) Hybrid Single-Particle Lagrangian Integrated Trajectory (HYSPLIT) model (version 4) (Draxler and Rolph, 2012; Rolph, 2012, http://www.arl.noaa.gov/ready/hysplit4.html). In addition, O_3 and PAN concentrations were calculated using a global chemistry model, the Community Atmosphere Model with

Chemistry (CAM-Chem), a component of the Community Earth System Model (CESM) (Lamarque et al., 2012; Tilmes et al., 2015). The CAM-chem results shown here follow the configuration used for the HTAP2 (Hemispheric Transport of Air Pollution, Phase 2) intercomparison (e.g., Stjern et al., 2016). CAM-chem is nudged to observed meteorology (GEOS-5) to reproduce the actual period of the observations (Oct 2010). The emissions used in the model are the HTAP2 inventory (Janssens-Maenhout, et al., 2015), which include the "MIX" Asian emissions inventory. Biomass burning emissions are from the Global Fire Emissions Database (GFED3) (Randerson et al., 2013).

3. Results

In the present experiments, PAN concentrations range from 0.1 to 2.4 ppbv, with an average of 0.6 ppbv. This mean value is lower than those observed in other Asian megacities: Beijing (1.41 ppb in the summer), Pearl River Delta region (1.32 ppb in the summer), and Seoul (0.8 ppb in the early summer); similar to those of suburban areas in China, e.g., Lanzhou (0.76 ppb in the summer); and higher than those of urban and rural sites in Japan, e.g., Tokyo (up to 0.6 ppb in the fall), Rishiri Island (~0.5 ppb in spring) or in the western coast of the US, e.g., Sacramento (0.45 ppb in the summer), Mt. Bachelor (0.144 ppb in the spring and early summer), off the western coast of the US (0.65 ppb in the spring), and over the remote North Pacific (total PAN < 0.3 ppb in spring) (Bertram et al., 2013; Fischer et al., 2011; La Franchi et al., 2009; Lee et al., 2008; Roberts et al., 2004; Tanimoto et al., 1999; Tanimoto et al., 2002; Wang et al., 2010; Zhang et al., 2009; Zhang et al., 2011). Because the PAN lifetime is greatly dependent on temperature, its concentration decreases with increasing distance from the source regions. The PAN concentrations calculated in this study thus lie in-between the levels for the East Asian megacities and the northern Pacific. The distributions of

all measured species, including PAN and O_3, are presented in Fig. 1. In particular, there are several periods characterized by high concentrations of PAN, O_3, and $PM_{2.5}$. In terms of PAN, four periods are particularly interesting (Fig. 1). High O_3 concentrations were observed during October 31–November 2 [episode 1] but did not coincide with high PAN concentrations. During October 28–29 [episode 2], NO_2 was noticeably increased. On the other hand, PAN and O_3 concentrations were both high during October 20–21 [episode 3] and November 4–5 [episode 4]. Episodes 3 and 4 are characterized by haze, while episodes 1 and 2 are characterized by urban influence in the Korean and Beijing outflows, respectively. Haze is reported by Korea Meteorological Administration (KMA) as a meteorological phenomenon when visibility is 1~ 10 km and relative humidity is less than 75 %.

In the present study, PAN correlates reasonably well with O_3 (γ = 0.67) and even better with $PM_{2.5}$ (γ = 0.79). In general, O_3 and PAN exhibit typical diurnal variation with a maximum recorded in the afternoon, which results in a good correlation between the two (Brasseur et al., 1999; Gaffney et al., 1999; Ridley et al., 1990; Schrimpf et al., 1995; Wang et al., 2010). In this study, however, the O_3 peak was often found in the early morning and late afternoon for several days (Fig. 1). Observing the diurnal variations in the entire PAN concentration measurement set (Fig. 2), the maximum was clearly recorded in the morning with the highest outliers, which is rather similar to that of $PM_{2.5}$. The diurnal pattern of NO_2 shows little variation, even though its concentrations were increased in the morning along with PAN. This first measurement of PAN at GCO reveals that PAN is not always coupled with O_3, which was not typically observed at remote sites in previous studies (e.g., Fischer et al., 2010; Lee et al., 2012).

4. Discussion

4.1. Decoupling of PAN from O_3

To examine the detailed mechanism of the decoupling of PAN from O_3, the daily maximum concentrations of PAN and O_3 were further explored. The recorded daily PAN maxima were generally in good correlation with O_3, albeit the relationship did not seem to hold at high concentrations of PAN and O_3 (Fig. 3). The daily maxima were then categorized into four groups according to the time when each O_3 and PAN maximum was recorded: "O_3 day-PAN day," "O_3 day-PAN night," "O_3 night-PAN day," and "O_3 night-PAN night." The day interval started from 08:00 and ended at 18:00 (local time), based on the times of sunrise and sunset during the experiment period. While the high PAN concentrations were associated with the "O_3 day-PAN day" group (cross symbols in Fig. 3), the enhanced O_3 concentration was recorded in the "O_3 night-PAN night" group (star symbols in Fig. 3). The "O_3 night-PAN night" group unexpectedly held more data points than the "O_3 day-PAN day" group, even though the "O_3 night-PAN night" group concentrations were lower (Fig. 3). In addition, there were several days classified in the "O_3 night-PAN day" (marked by diamond) and "O_3 day-PAN night" groups, but with less frequency and lower concentrations. These results indicate that the decoupling of PAN from O_3 was primarily due to the elevated concentrations of O_3 and PAN at night. While PAN reached the maximum during the day on Oct 20 and Nov 5, their concentrations were increased from the previous day through the night. The four high PAN and O_3 episodes identified in this study fall under the category of "O_3 night-PAN night" or "O_3 day-PAN day". These two cases will be further examined to identify the chemical and physical processes responsible for PAN being decoupled from O_3, instead of being coupled with $PM_{2.5}$. The overall characteristics of the four episodes are summarized in Table 1.

4.2. Export of O_3 from Asian continents (episodes 1 & 2)

High O_3 concentrations were encountered around midnight on three consecutive days from

October 31 to November 2 (episode 1), during which SO_2 reached its maximum concentration (Fig. 1). The backward trajectories of air masses revealed that air passed through the Beijing area during this period (Fig. 4). The wind was strong (13.5 m/s on average) and the recorded O_3 maximum (80.6 ppbv) was concurrent with the PAN maximum (0.9 ppbv) around midnight on November 1st (Fig. 1).

All these results indicate that the air was heavily influenced by outflow from the Beijing area, as previously hypothesized (Lim et al., 2012), and that the nighttime enhancement of O_3 and PAN resulted from the fast transport of relatively less-aged urban plumes. Because the overall correlation between O_3 and PAN was the best with the highest daily $\Delta O_3/\Delta PAN$ among all cases discussed in this study, episode 1 likely represents an event of rapid transport from the Beijing area (Fig. 5a).

In previous studies, the nighttime enhancement of O_3 was observed at GCO (e.g., Lee et al., 2007) in association with pollutant-laden air coming from Beijing. Similarly, Banta et al. (1998) pointed out that the evening O_3 maximum was due to long-range transport of O_3 from nearby urban areas. Wang et al. (2011) reported that the O_3 lifetime was about two days in East China during the summer, which is sufficient time for air to travel to GCO. Therefore, the nighttime maximum of O_3 can be attributed to the export of O_3 from megacities in China. It causes PAN to be decoupled from O_3 because PAN levels remained low, even though there was good correlation between the two species. Another night maximum of O_3 was recorded on October 29. Note that NO_x was highly elevated during October 28–29 (episode 2) (Fig. 1). However, O_3 level was relatively low, leading to the lowest daily $\Delta O_3/\Delta PAN$ among all episodes. In this case, air masses passed through the Korean Peninsula, carrying low O_3 being titrated by high NO_x (Brasseur et al., 1999; Jacobson, 2005). These two urban plumes are well contrasted in terms of O_3 and NO_x levels (Table 1), depending on the degree of aging.

4.3. PAN enhancement upon occurrence of haze (episodes 3 & 4)

In this study, two haze events were observed in the very beginning (October 20–21; episode 3) and the end of the study period (November 4–5; episode 4). As the nighttime O_3 peak was attributed to the transport from nearby urban areas to Jeju Island, the two haze episodes were also observed in association with continental outflows. The first haze event occurred on October 18th and lingered until October 21st, during which O_3 concentrations were gradually elevated. A second peak was recorded around midnight of October 19th and 20th, and the maximum was reached in the afternoon of October 20th (Figs. 1 and 3). In this episode, the maximum concentrations of O_3 and PAN were 78.9 ppbv and 2.0 ppbv, respectively, on October 29th, when the highest NO_2 concentration (12.7 ppbv) was observed under low wind speed (6.6 m/s daily average). The air mass trajectories suggest the influence of the Korean Peninsula, particularly the Seoul metropolitan area, in addition to East China (Fig. 4).

In the second haze event (episode 4), an air mass was slowly transported from East China, including the Jiangsu province, under stagnant condition which was developed by an anticyclone system (Fig. 4). We measured the highest concentrations of all aerosol species including the $PM_{2.5}$ mass as well as PAN and O_3, which were 156 $\mu g/m^3$, 2.4 ppbv, and 87.5 ppbv, respectively. Other reactive gases such as CO, SO_2, and NO_2 were also highly elevated. Note that PAN and O_3 gradually increased through the night, leading to a nighttime maximum of both species on November 4th. It is likely that the pre-formed PAN and O_3 were continuously transported into Gosan at night.

PAN is formed through the reaction of the peroxyacetyl radical and nitrogen dioxide (Eq. 1) and decomposed at high temperature (Eq. 2), returning these radicals. Unless the NO

concentration is high (Eq. 3), the peroxyacetyl radical recombines with NO_2, producing PAN. Thus, the total lifetime of PAN depends on the NO_2/NO ratio and temperature (Eq. 4) (Brasseur et al., 1999).

$$CH_3C(O)O_2 + NO_2 + M \rightarrow PAN + M \quad (1)$$

$$PAN \rightarrow CH_3C(O)O_2 + NO_2 \quad (2)$$

$$CH_3C(O)O_2 + NO \rightarrow CH_3CO_2 + NO_2 \quad (3)$$

$$T_{eff} = T_d \left(1 + \frac{k_1[NO_2]}{k_2[NO]}\right) \ [sec^{-1}] \quad (4)$$

where T_d and T_{eff} indicate the lifetime against decomposition and the effective lifetime of PAN (Brasseur et al., 1999). The effective lifetime of PAN was estimated through Eq. 4 using the rate constants proposed by Brasseur et al. (1999), Jacobson (2005), and Maricq and Szente (1996).

During the haze event, NO was close to the detection limit, while NO_2 was greatly enhanced. Owing to the high NO_2/NO ratio, the effective lifetime of PAN increased by 57 times; this possibly contributed to the gradual increase in PAN through the night on November 4th. Fischer et al. (2014) also reported that, at night, PAN can be produced from the reaction of acetaldehyde with the nitrate radical.

Besides $PM_{2.5}$, PAN was also well correlated with $PM_{2.5}$ OC and EC not only during this haze episode but also during the entire measurement period (Fig. 6a and b). Furthermore, the enhancement of PAN was concurrent with that of OC and K^+, resulting in excellent correlation between them (Fig. 6b and d). In fact, the ΔOC/ΔEC ratio of episode 4 was much higher (7) than those of the other episodes (~2.5) (Fig. 6c). The fraction of $PM_{2.5}$ against $PM_{2.5}$ was also the highest in this episode, indicating significant contribution of secondary aerosols. These observations suggest that air masses were affected by biomass combustion (e.g., Ram et al., 2008, 2012; Saarikoski et al., 2008).

According to previous studies, PAN can be produced in plumes through biomass

288 combustion (Alvarado et al., 2010; Coheur et al., 2007; Liu et al., 2016b; Tereszchuk et al.,
289 2013). In northeast China, open burnings related to agricultural activities frequently occur
290 during the spring and fall (Duan et al., 2004; Yang et al., 2005). Kudo et al. (2014) also
291 reported that, upon burning crop residue in Yangtze region, the levels of oxygenated VOCs
292 were elevated together with NO_x. In addition, biofuel is used for cooking and heating and as
293 an energy source in China's industry (Cao et al., 2006).

294 Therefore, PAN is likely to increase when haze occurs and fine aerosols are transformed as
295 air masses carrying combustion emissions are slowly transported from China over the Yellow
296 Sea. Additionally, the results of this study imply that PAN can be used as a robust tracer for
297 continental outflows in northeast Asia, to identify transport- and chemical transformation-
298 dominant regimes. In a transport-dominant regime, O_3 export was distinguished by the
299 highest levels of primary gaseous species such as SO_2 and relatively low levels of PAN. In
300 contrast, fine aerosol species are enhanced in a chemical transformation regime, leading to
301 haze events with relatively more enhanced PAN compared to O_3.

302 Finally, the measured O_3 and PAN concentrations were compared to results from a global
303 chemistry model CAM-Chem. In the model simulation, O_3 and PAN were highly
304 underestimated during the episodes observed in Chinese outflows, although the variation
305 around average level of O_3 and PAN was well captured (Fig. 7). The elevated PAN
306 concentration was underestimated in the model (Oct 20–21 and Nov 4–5), especially when air
307 was impacted by biomass combustion. The timing of the O_3 diurnal variability was captured
308 by the model, although the magnitude of the variation was underestimated. These results
309 reveal that the current understanding of Chinese outflow is still not sufficient, thereby causing
310 uncertainty in estimating its effect on air quality in the northwestern Pacific Rim.

5. Conclusions

The first measurements of PAN, reactive gases, and aerosol species were conducted at GCO during October 19 to November 6, 2010. The average concentration of PAN was 0.6 ppbv with a maximum of 2.4 ppbv, which was lower than those in major cities in East Asia but much higher than the background concentrations in other regions. In addition, PAN and O_3 concentrations were well correlated (γ = 0.67). However, the comparison of the daily maxima of PAN and O_3 highlighted that they were not proportionally enhanced. That is, either PAN was relatively more elevated than O_3 or the highest O_3 was associated with low levels of PAN. Unexpectedly, both PAN and O_3 often reached their maxima at night. As a result, PAN was decoupled from O_3 and better correlated with the $PM_{2.5}$ mass (γ = 0.79) than with O_3. In this study, these high-concentration episodes were all encountered in association with continental outflows, and thus, two high-O_3 and two high-PAN events were recorded and investigated in detail.

During the O_3 episodes, both O_3 and PAN concentrations reached their maximum values at night. In episode 1 (Oct. 31 to Nov. 2), the O_3 concentration was increased to 80.6 ppbv, with a high SO_2 concentration under strong wind. It was a typical Beijing plume observed in the study region. In comparison, NO_2 was greatly increased in episode 2 (Oct. 28–29) when the air masses were affected by urban emissions from Korean Peninsula. Although the maximum O_3 level was lower during episode 2, these two cases demonstrated well how O_3 was exported from the East Asian continent.

The remaining two episodes were highlighted by enhanced PAN concentrations and characterized by haze occurrence. During episode 3 (Oct. 20–21), PAN and O_3 concentrations increased up to 2.0 ppbv and 78.9 ppbv, respectively, with high NOx levels, probably influenced by emissions from Korea. Episode 4 (Nov. 4–5) was characterized by the highest

concentrations of almost all measured species, including PAN, O_3, $PM_{2.5}$ mass, and $PM_{1.0}$ species; the maximum recorded concentrations of PAN, O_3, and $PM_{2.5}$ mass during this interval were 2.4 ppbv, 87.5 ppbv, and 156 $\mu g/m^3$, respectively. Note that, along with $PM_{2.5}$ and O_3, PAN was gradually increased through the night. In this episode, an air mass was slowly transported from eastern China. With depleted NO, the effective lifetime of PAN was greatly extended. In addition, PAN concentration showed good correlation with OC, EC, and K^+; in fact, the correlation of PAN with K^+ was comparable to that of OC with K^+. These results, in conjunction with the high $\Delta OC/EC$ (7), imply that the observed haze was mainly caused by the emissions produced by biomass combustion. These results suggest that PAN is a useful tool for distinguishing continental outflows that were typically observed in northeast Asia.

The comparison between the measured and calculated concentrations using the CAM-Chem-HTAP2 model showed that the model underestimated the O_3 and PAN levels in Chinese outflows, particularly for haze incidence. These results reveal that Chinese outflows are still poorly understood and not well captured in the model.

Acknowledgments

This study was funded by the Korea Meteorological Administration Research and Development Program under Grant KMIPA 2015-6020. The National Center for Atmospheric Research is funded by the National Science Foundation. The authors gratefully acknowledge the NOAA Air Resources Laboratory (ARL) for the provision of the HYSPLIT transport and dispersion model and/or READY website (http://www.ready.noaa.gov) used in this publication.

References

Akimoto, H.: Global air quality and pollution, Science, 302, 1716-1719, doi:10.1126/science.1092666, 2003.

Alvarado, M. J., Logan, J. A., Mao, J., Apel, E., Riemer, D., Blake, D., Cohen, R. C., Min, K. E., Perring, A. E., Browne, E. C., Wooldridge, P. J., Diskin, G. S., Sachse, G. W., Fuelberg, H., Sessions, W. R., Harrigan, D. L., Huey, G., Liao, J., Case-Hanks, A., Jimenez, J. L., Cubison, M. J., Vay, S. A., Weinheimer, A. J., Knapp, D. J., Montzka, D. D., Flocke, F. M., Pollack, I. B., Wennberg, P. O., Kurten, A., Crounse, J., Clair, J. M. S., Wisthaler, A., Mikoviny, T., Yantosca, R. M., Carouge, C. C., and Le Sager, P.: Nitrogen oxides and PAN in plumes from boreal fires during ARCTAS-B and their impact on ozone: an integrated analysis of aircraft and satellite observations, Atmos. Chem. Phys., 10, 9739-9760, doi:10.5194/acp-10-9739-2010, 2010.

Aneja, V. P., Hartsell, B. E., Kim, D. S., and Grosjean, D.: Peroxyacetyl nitrate in Atlanta, Georgia: Comparison and analysis of ambient data for suburban and downtown locations, J. Air & Waste Manage. Assoc., 49, doi: 177-184, 10.1080/10473289.1999.10463786, 1999.

Banta, R. M., Senff, C. J., White, A. B., Trainer, M., McNider, R. T., Valente, R. J., Mayor, S. D., Alvarez, R. J., Hardesty, R. M., Parrish, D., and Fehsenfeld, F. C.: Daytime buildup and nighttime transport of urban ozone in the boundary layer during a stagnation episode, J. Geophys. Res. Atmos., 103, 22519-22544, doi:10.1029/98jd01020, 1998.

Beine, H. J., Jaffe, D. A., Herring, J. A., Kelley, J. A., Krognes, T., and Stordal, F.: High-latitude springtime photochemistry .1. NOx, PAN and ozone relationships, J. Atmos. Chem., 27, 127-153, doi:10.1023/a:1005869900567, 1997.

Bertram, T. H., Perring, A. E., Wooldridge, P. J., Dibb, J., Avery, M. A., and Cohen, R. C.: On the export of reactive nitrogen from Asia: NO_x partitioning and effects on ozone, Atmos. Chem. Phys., 13, 4617-4630, doi:10.5194/acp-13-4617-2013, 2013.

Brasseur, G. P., Orlando, J. J., and Tyndall, G. S.: Atmospheric chemistry and global change, Oxford University Press, New York, 235-347 pp., 1999.

Cao, G., Zhang, X., and Zheng, F.: Inventory of black carbon and organic carbon emissions from China, Atmos. Environ., 40, 6516-6527, doi:10.1016/j.atmosenv.2006.05.070, 2006.

Coheur, P. F., Herbin, H., Clerbaux, C., Hurtmans, D., Wespes, C., Carleer, M., Turquety, S., Rinsland, C. P., Remedios, J., Hauglustaine, D., Boone, C. D., and Bernath, P. F.: ACE-FTS observation of a young biomass burning plume: first reported measurements of C_2H_4, C_3H_6O, H_2CO and PAN by infrared occultation from space, Atmos. Chem. Phys., 7, 5437-5446, doi:10.5194/acp-7-5437-2007, 2007.

Draxler, R. R., and Rolph, G. D.: HYSPLIT (HYbrid Single-Particle Lagrangian Integrated Trajectory) Model access via NOAA ARL READY Website (http://ready.arl.noaa.gov/HYSPLIT.php), NOAA Air Resources Laboratory, Silver Spring, MD., 2012.

Duan, F., Liu, X., Yu, T., and Cachier, H.: Identification and estimate of biomass burning contribution to the urban aerosol organic carbon concentrations in Beijing, Atmos. Environ., 38, 1275-1282, doi:10.1016/j.atmosenv.2003.11.037, 2004.

401 Fischer, E. V., Jaffe, D. A., Reidmiller, D. R., and Jaeglé, L.: Meteorological controls on
402 observed peroxyacetyl nitrate at Mount Bachelor during the spring of 2008, J. Geophys.
403 Res., 115, D03302, doi:10.1029/2009jd012776, 2010.

404 Fischer, E. V., Jaffe, D. A., and Weatherhead, E. C.: Free tropospheric peroxyacetyl nitrate
405 (PAN) and ozone at Mount Bachelor: potential causes of variability and timescale for
406 trend detection, Atmos. Chem. Phys., 11, 5641-5654, doi:10.5194/acp-11-5641-2011,
407 2011.

408 Fischer, E. V., Jacob, D. J., Yantosca, R. M., Sulprizio, M. P., Millet, D. B., Mao, J., Paulot, F.,
409 Singh, H. B., Roiger, A., Ries, L., Talbot, R. W., Dzepina, K., and Pandey, D. S.:
410 Atmospheric peroxyacetyl nitrate (PAN): a global budget and source attribution, Atmos.
411 Chem. Phys., 14, 2679-2698, doi:10.5194/acp-14-2679-2014, 2014.

412 Gaffney, J. S., Fajer, R., and Senum, G. I.: An improved procedure for high purity gaseous
413 peroxyacyl nitrate production: Use of heavy lipid solvents, Atmos. Environ., 18, 215-
414 218, doi:10.1016/0004-6981(84)90245-2, 1984.

415 Gaffney, J. S., Bornick, R. M., Chen, Y. H., and Marley, N. A.: Capillary gas chromatographic
416 analysis of nitrogen dioxide and pans with luminol chemiluminescent detection, Atmos.
417 Environ., 32, 1445-1454, doi:10.1016/S1352-2310(97)00098-8, 1998.

418 Gaffney, J. S., Marley, N. A., Cunningham, M. M., and Doskey, P. V.: Measurements of
419 peroxyacyl nitrates (PANs) in Mexico City: implications for megacity air quality
420 impacts on regional scales, Atmos. Environ., 33, 5003-5012, doi:10.1016/S1352-
421 2310(99)00263-0, 1999.

422 Gallagher, M. S., Carsey, T. P., and Farmer, M. L.: Peroxyacetyl nitrate in the North Atlantic
423 marine boundary layer, Global Biogeochem. Cycle., 4, 297-308,
424 doi:10.1029/GB004i003p00297, 1990.

425 Gregory, G. L.: An intercomparison of airborne PAN measurements, J. Geophys. Res., 95,
426 10077-10087, doi:10.1029/JD095iD07p10077, 1990.

427 Grosjean, E., Grosjean, D., Woodhouse, L. F., and Yang, Y.-J.: Peroxyacetyl nitrate and
428 peroxypropionyl nitrate in Porto Alegre, Brazil, Atmos. Environ., 36, 2405-2419,
429 doi:10.1016/S1352-2310(01)00541-6, 2002.

430 Gu, D., Wang, Y., Smeltzer, C., and Liu, Z.: Reduction in NOx Emission Trends over China:
431 Regional and Seasonal Variations, Environ. Sci. Technol., 47, 12912–12919,
432 doi:10.1021/es401727e, 2013.

433 Hansel, A., and Wisthaler, A.: A method for real-time detection of PAN, PPN and MPAN in
434 ambient air, Geophys. Res. Lett., 27, 895-898, doi:10.1029/1999gl010989, 2000.

435 Jacob, D. J.: Introduction to atmospheric chemistry, 199-231 pp., 1999.

436 Jacob, D. J.: Heterogeneous chemistry and tropospheric ozone, Atmos. Environ., 34, 2131-
437 2159, doi:10.1016/s1352-2310(99)00462-8, 2000.

438 Jacobson, M. Z.: Fundamentals of atmospheric modeling, Second edition, Cambridge, UK,
439 731-738 pp., 2005.

440 Jaffe, D. A., Thornton, J., Wolfe, G., Reidmiller, D., Fischer, E. V., Jacob, D. J., Zhang, L.,
441 Cohen, R., Singh, H., Weinheimer, A., and Flocke, F.: Can we detect an Influence over
442 North America from Increasing Asian NOx Emissions?, Eos Trans, AGU, 88, 2007.

Janssens-Maenhout, G., Crippa, M., Guizzardi, D., Dentener, F., Muntean, M., Pouliot, G., Keating, T., Zhang, Q., Kurokawa, J., Wankmüller, R., Denier van der Gon, H., Kuenen, J. J. P., Klimont, Z., Frost, G., Darras, S., Koffi, B., and Li, M.: HTAP_v2.2: a mosaic of regional and global emission grid maps for 2008 and 2010 to study hemispheric transport of air pollution, Atmos. Chem. Phys., 15, 11411-11432, doi:10.5194/acp-15-11411-2015, 2015.

Jung, M., Variations of HONO at Gosan in March, 2011, master thesis, Korea University, 2013.

Kanaya, Y., Tanimoto, H., Matsumoto, J., Furutani, H., Hashimoto, S., Komazaki, Y., Tanaka, S., Yokouchi, Y., Kato, S., Kajii, Y., and Akimoto, H.: Diurnal variations in H_2O_2, O_3, PAN, HNO_3 and aldehyde concentrations and NO/NO_2 ratios at Rishiri Island, Japan: Potential influence from iodine chemistry, Sci. Total Envir., 376, 185-197, doi:10.1016/j.scitotenv.2007.01.073, 2007.

Kenley, R. A., and Hendry, D. G.: Generation of peroxy radicals from peroxynitrates ($ROONO_2$). Decomposition of peroxybenzoyl nitrate (PBzN), J. Am. Chem. Soc., 104, 220-224, doi:10.1021/ja00365a040, 1982.

Kourtidis, K. A., Fabian, P., Zerefos, C., and RappenglÜCk, B.: Peroxyacetyl nitrate (PAN), peroxypropionyl nitrate (PPN) and PAN/ozone ratio measurements at three sites in Germany, Tellus B, 45, 442-457, doi:10.1034/j.1600-0889.1993.t01-3-00004.x, 1993.

Krotkov, N. A., McLinden, C. A., Li, C., Lamsal, L. N., Celarier, E. A., Marchenko, S. V., Swartz, W. H., Bucsela, E. J., Joiner, J., Duncan, B. N., Boersma, K. F., Veefkind, J. P., Levelt, P. F., Fioletov, V. E., Dickerson, R. R., He, H., Lu, Z., and Streets, D. G.: Aura OMI observations of regional SO2 and NO2 pollution changes from 2005 to 2015, Atmos. Chem. Phys., 16, 4605–4629, doi:10.5194/acp-16-4605-2016, 2016.

Kudo, S., Tanimoto, H., Inomata, S., Saito, S., Pan, X., Kanaya, Y., Taketani, F., Wang, Z., Chen, H., Dong, H., Zhang, M., and Yamaji, K.: Emissions of nonmethane volatile organic compounds from open crop residue burning in the Yangtze River Delta region, China, J. Geophys. Res., 119, 7684–7698, doi:10.1002/2013JD021044, 2014.

LaFranchi, B. W., Wolfe, G. M., Thornton, J. A., Harrold, S. A., Browne, E. C., Min, K. E., Wooldridge, P. J., Gilman, J. B., Kuster, W. C., Goldan, P. D., De Gouw, J. A., McKay, M., Goldstein, A. H., Ren, X., Mao, J., and Cohen, R. C.: Closing the peroxy acetyl nitrate budget: Observations of acyl peroxy nitrates (PAN, PPN, and MPAN) during BEARPEX 2007, Atmos. Chem. Phys., 9, 7623-7641, doi:10.5194/acp-9-7623-2009, 2009.

Lamarque, J. F., Emmons, L. K., Hess, P. G., Kinnison, D. E., Tilmes, S., Vitt, F., Heald, C. L., Holland, E. A., Lauritzen, P. H., Neu, J., Orlando, J. J., Rasch, P. J., and Tyndall, G. K.: CAM-chem: description and evaluation of interactive atmospheric chemistry in the Community Earth System Model, Geosci. Model Dev., 5, 369-411, doi:10.5194/gmd-5-369-2012, 2012.

Lee, G., Jang, Y., Lee, H., Han, J.-S., Kim, K.-R., and Lee, M.: Characteristic behavior of peroxyacetyl nitrate (PAN) in Seoul megacity, Korea, Chemosphere, 73, 619-628, doi:10.1016/j.chemosphere.2008.05.060, 2008.

Lee, G., Choi, H.-S., Lee, T., Choi, J., Park, J. S., and Ahn, J. Y.: Variations of regional background peroxyacetyl nitrate in marine boundary layer over Baengyeong Island,

South Korea, Atmos. Environ., 61, 533-541, doi:10.1016/j.atmosenv.2012.07.075, 2012.

Lee, M., Song, M., Moon, K. J., Han, J. S., Lee, G., and Kim, K.-R.: Origins and chemical characteristics of fine aerosols during the northeastern Asia regional experiment (Atmospheric Brown Cloud-East Asia Regional Experiment 2005), J. Geophys. Res., 112, D22S29, doi:10.1029/2006jd008210, 2007.

Li, M., Zhang, Q., Kurokawa, J., Woo, J. H., He, K. B., Lu, Z., Ohara, T., Song, Y., Streets, D. G., Carmichael, G. R., Cheng, Y. F., Hong, C. P., Huo, H., Jiang, X. J., Kang, S. C., Liu, F., Su, H., and Zheng, B.: MIX: a mosaic Asian anthropogenic emission inventory for the MICS-Asia and the HTAP projects, Atmos. Chem. Phys. Discuss., 2015, 34813-34869, doi:10.5194/acpd-15-34813-2015, 2015.

Lim, S., Lee, M., Lee, G., Kim, S., Yoon, S., and Kang, K.: Ionic and carbonaceous compositions of PM_{10}, $PM_{2.5}$ and $PM_{1.0}$ at Gosan ABC Superstation and their ratios as source signature, Atmos. Chem. Phys., 12, 2007-2024, doi:10.5194/acp-12-2007-2012, 2012.

Liu, F., Zhang, Q., A., van der A, R. J., Zheng, B., Tong, D., Yan, L., Zheng, Y., and He, K.: Recent reduction in NO x emissions over China: synthesis of satellite observations and emission inventories, Environmental Research Letters, 11, 114002, doi:10.1088/1748-9326/11/11/114002, 2016a.

Liu, Z., Wang, Y., Gu, D., Zhao, C., Huey, L. G., Stickel, R., Liao, J., Shao, M., Zhu, T., Zeng, L., Liu, S.-C., Chang, C.-C., Amoroso, A., and Costabile, F.: Evidence of reactive aromatics as a major source of peroxy acetyl nitrate over China, Environ. Sci. Technol., 44, 7017-7022, doi:10.1021/es1007966, 2010.

Liu, X., Zhang, Y., Huey, L. G., Yokelson, R. J., Wang, Y., Jimenez, J. L., Campuzano-Jost, P., Beyersdorf, A. J., Blake, D. R., Choi, Y., St. Clair, J. M., Crounse, J. D., Day, D. A., Diskin, G. S., Fried, A., Hall, S. R., Hanisco, T. F., King, L. E., Meinardi, S., Mikoviny, T., Palm, B. B., Peischl, J., Perring, A. E., Pollack, I. B., Ryerson, T. B., Sachse, G., Schwarz, J. P., Simpson, I. J., Tanner, D. J., Thornhill, K. L., Ullmann, K., Weber, R. J., Wennberg, P. O., Wisthaler, A., Wolfe, G. M., and Ziemba, L. D.: Agricultural fires in the southeastern U.S. during SEAC4RS: Emissions of trace gases and particles and evolution of ozone, reactive nitrogen, and organic aerosol, J. Geophys, Res.- Atmos., 121, 7383-7414, doi:10.1002/2016JD025040, 2016b.

Maricq, M. M., and Szente, J. J.: Temperature-dependent study of the $CH_3C(O)O_2$ + NO reaction, J. Phys. Chem., 100, 12380-12385, doi:10.1021/jp960792c, 1996.

Marley, N. A., Gaffney, J. S., White, R. V., Rodriguez-Cuadra, L., Herndon, S. E., Dunlea, E., Volkamer, R. M., Molina, L. T., and Molina, M. J.: Fast gas chromatography with luminol chemiluminescence detection for the simultaneous determination of nitrogen dioxide and peroxyacetyl nitrate in the atmosphere, Rev. Sci. Instr., 75, 4595-4605, doi:10.1063/1.1805271, 2004.

Mills, G. P., Sturges, W. T., Salmon, R. A., Bauguitte, S. J. B., Read, K. A., and Bandy, B. J.: Seasonal variation of peroxyacetylnitrate (PAN) in coastal Antarctica measured with a new instrument for the detection of sub-part per trillion mixing ratios of PAN, Atmos. Chem. Phys., 7, 4589-4599, doi:10.5194/acp-7-4589-2007, 2007.

Muller, K. P., and Rudolph, J.: Measurements of peroxyacetylnitrate in the marine boundary layer over the Atlantic, J. Atmos. Chem., 15, 361-367, doi:10.1007/BF00115405, 1992.

Nielsen, T., Samuelsson, U., Grennfelt, P., and Thomsen, E. L.: Peroxyacetyl nitrate in long-range transported polluted air, Nature, 293, 553-555, doi:10.1038/293553a0, 1981.

NIER, Annual Report of Ambient Air Quality in Korea, 2015, National Institute of Environmental Research, Inchon, Korea, 350pp., 2016a (in Korean).

NIER, Guidelines for installation and operation of air pollution monitoring network, National Institute of Environmental Research, Inchon, Korea, 427 pp., 2016b (in Korean).

Ohara, T., Akimoto, H., Kurokawa, J., Horii, N., Yamaji, K., Yan, X., and Hayasaka, T.: An Asian emission inventory of anthropogenic emission sources for the period 1980-2020, Atmos. Chem. Phys., 7, 4419-4444, doi:10.5194/acp-7-4419-2007, 2007.

Ram, K., Sarin, M. M., and Hegde, P.: Atmospheric abundances of primary and secondary carbonaceous species at two high-altitude sites in India: Sources and temporal variability, Atmos. Environ., 42, 6785-6796, doi:10.1016/j.atmosenv.2008.05.031, 2008.

Ram, K., Sarin, M. M., and Tripathi, S. N.: Temporal trends in atmospheric $PM_{2.5}$, PM_{10}, elemental carbon, organic carbon, water-soluble organic carbon, and optical properties: Impact of biomass burning emissions in the Indo-Gangetic Plain, Environ. Sci. Technol., 46, 686-695, doi:10.1021/es202857w, 2012.

Randerson, J. T., van der Werf, G. R., Giglio, L., Collatz, G. J., and Kasibhatla, P. S.: Global Fire Emissions Database, Version 3 (GFEDv3.1). Data set. Available on-line [http://daac.ornl.gov/] from Oak Ridge National Laboratory Distributed Active Archive Center, Oak Ridge, Tennessee, USA. doi:10.3334/ORNLDAAC/1191, 2013.

Ridley, B. A., Shetter, J. D., Gandrud, B. W., Salas, L. J., Singh, H. B., Carroll, M. A., Hubler, G., Albritton, D. L., Hastie, D. R., Schiff, H. I., Mackay, G. I., Karechi, D. R., Davis, D. D., Bradshaw, J. D., Rodgers, M. O., Sandholm, S. T., Torres, A. L., Condon, E. P., Gregory, G. L., and Beck, S. M.: Ratios of peroxyacetyl nitrate to active nitrogen observed during aircraft flights over the Eastern Pacific Oceans and continental United-States, J. Geophys. Res., 95, 10179-10192, doi:10.1029/JD095iD07p10179, 1990.

Roberts, J. M., Flocke, F., Chen, G., de Gouw, J., Holloway, J. S., Hübler, G., Neuman, J. A., Nicks, D. K., Nowak, J. B., Parrish, D. D., Ryerson, T. B., Sueper, D. T., Warneke, C., and Fehsenfeld, F. C.: Measurement of peroxycarboxylic nitric anhydrides (PANs) during the ITCT 2K2 aircraft intensive experiment, J. Geophys, Res.- Atmos., 109, D23S21, doi:10.1029/2004JD004960, 2004.

Roberts, J. M., Marchewka, M., Bertman, S. B., Sommariva, R., Warneke, C., de Gouw, J., Kuster, W., Goldan, P., Williams, E., Lerner, B. M., Murphy, P., and Fehsenfeld, F. C.: Measurements of PANs during the New England Air Quality Study 2002, J. Geophys. Res., 112, D20306, doi:10.1029/2007JD008667, 2007.

Rolph, G. D.: Real-time Environmental Applications and Display sYstem (READY) Website (http://ready.arl.noaa.gov). NOAA Air Resources Laboratory, Silver Spring, MD. , 2012.

Saarikoski, S., Timonen, H., Saarnio, K., Aurela, M., Ärvi, L., Keronen, P., Kerminen, V. M., and Hillamo, R.: Sources of organic carbon in fine particulate matter in northern European urban air, Atmos. Chem. Phys., 8, 6281-6295, doi:10.5194/acp-8-6281-2008, 2008.

Schrimpf, W., Muller, K. P., Johnen, F. J., Lienaerts, K., and Rudolph, J.: An optimized method for airborne peroxyacetyl nitrate (PAN) measurements, J. Atmos. Chem., 22,

303-317, doi:10.1007/bf00696640, 1995.

Shang, X., Lee, M., Han, J., Kang, E., Gustafsson, Ö., and Chang, L.-S.: Identifiction and chemical characteristics of distinctive Chinese outflow plumes associated with enhanced submicron aerosols at Gosan Climate Observatory, submitted at Aerosol Air Qual. Res.

Staudt, A. C., Jacob, D. J., Ravetta, F., Logan, J. A., Bachiochi, D., Sandholm, S., Ridley, B., Singh, H. B., and Talbot, B.: Sources and chemistry of nitrogen oxides over the tropical Pacific, J. Geophys. Res., 108, 8239, doi:10.1029/2002JD002139, 2003.

Stjern, C. W., Samset, B. H., Myhre, G., Bian, H., Chin, M., Davila, Y., Dentener, F., Emmons, L., Flemming, J., Haslerud, A. S., Henze, D., Jonson, J. E., Kucsera, T., Lund, M. T., Schulz, M., Sudo, K., Takemura, T., and Tilmes, S.: Global and regional radiative forcing from 20% reductions in BC, OC and SO4 – an HTAP2 multi-model study, Atmos. Chem. Phys., 16, 13579-13599, doi:10.5194/acp-16-13579-2016, 2016.

Talukdar, R. K., Burkholder, J. B., Schmoltner, A. M., Roberts, J. M., Wilson, R. R., and Ravishankara, A. R.: Investigation of the loss processes for peroxyacetyl nitrate in the atmosphere: UV photolysis and reaction with OH, J. Geophys. Res., 100, 14163-14173, doi:10.1029/95JD00545, 1995.

Tanimoto, H., Hirokawa, J., Kajii, Y., and Akimoto, H.: A new measurement technique of peroxyacetyl nitrate at parts per trillion by volume levels: Gas chromatography/negative ion chemical ionization mass spectrometry, J. Geophys. Res., 104(17), 21, 343-21, 354, doi:10.1029/1999JD900345, 1999.

Tanimoto, H., H. Furutani, S. Kato, J. Matsumoto, Y. Makide, and H. Akimoto, Seasonal cycles of ozone and oxidized nitrogen species in northeast Asia, 1, Impact of regional climatology and photochemistry observed during RISOTTO 1999-2000, J. Geophys. Res., 107(D24), 4747, doi:10.1029/2001JD001496, 2002.

Tanimoto, H., K. Matsumoto, and M. Uematsu, Ozone–CO correlations in Siberian wildfire plumes observed at Rishiri Island, SOLA, 4, 65-68, doi:10.2151/sola.2008-017, 2008.

Tereszchuk, K. A., Moore, D. P., Harrison, J. J., Boone, C. D., Park, M., Remedios, J. J., Randel, W. J., and Bernath, P. F.: Observations of peroxyacetyl nitrate (PAN) in the upper troposphere by the Atmospheric Chemistry Experiment-Fourier Transform Spectrometer (ACE-FTS), Atmos. Chem. Phys., 13, 5601-5613, doi:10.5194/acp-13-5601-2013, 2013.

Tilmes, S., Lamarque, J. F., Emmons, L. K., Kinnison, D. E., Ma, P. L., Liu, X., Ghan, S., Bardeen, C., Arnold, S., Deeter, M., Vitt, F., Ryerson, T., Elkins, J. W., Moore, F., Spackman, J. R., and Val Martin, M.: Description and evaluation of tropospheric chemistry and aerosols in the Community Earth System Model (CESM1.2), Geosci. Model Dev., 8, 1395-1426, doi:10.5194/gmd-8-1395-2015, 2015.

Villena, G., Bejan, I., Kurtenbach, R., Wiesen, P., and Kleffmann, J.: Interferences of commercial NO_2 instruments in the urban atmosphere and in a smog chamber, Atmos. Meas. Tech., 5, 149-159, dio:10.5194/amt-5-149-2012, 2012.

Wang, B., Shao, M., Roberts, J. M., Yang, G., Yang, F., Hu, M., Zeng, L., Zhang, Y., and Zhang, J.: Ground-based on-line measurements of peroxyacetyl nitrate (PAN) and peroxypropionyl nitrate (PPN) in the Pearl River Delta, China, Int. J. Environ. Anal. Chem., 90, 548-559, doi:10.1080/03067310903194972, 2010.

Wang, Y., Zhang, Y., Hao, J., and Luo, M.: Seasonal and spatial variability of surface ozone over China: contributions from background and domestic pollution, Atmos. Chem. Phys., 11, 3511-3525, doi:10.5194/acp-11-3511-2011, 2011.

Yang, F., He, K., Ye, B., Chen, X., Cha, L., Cadle, S. H., Chan, T., and Mulawa, P. A.: One-year record of organic and elemental carbon in fine particles in downtown Beijing and Shanghai, Atmos. Chem. Phys., 5, 1449-1457, doi:10.5194/acp-5-1449-2005, 2005.

Zhang, H., Xu, X., Lin, W., and Wang, Y.: Wintertime peroxyacetyl nitrate (PAN) in the megacity Beijing: Role of photochemical and meteorological processes, J. Environ. Sci., 26, 83-96, doi:10.1016/S1001-0742(13)60384-8, 2014.

Zhang, J. B., Xu, Z., Yang, G., and Wang, B.: Peroxyacetyl nitrate (PAN) and peroxypropionyl nitrate (PPN) in urban and suburban atmospheres of Beijing, China, Atmos. Chem. Phys. Discuss., 11, 8173-8206, doi:10.5194/acpd-11-8173-2011, 2011.

Zhang, J. M., Wang, T., Ding, A. J., Zhou, X. H., Xue, L. K., Poon, C. N., Wu, W. S., Gao, J., Zuo, H. C., Chen, J. M., Zhang, X. C., and Fan, S. J.: Continuous measurement of peroxyacetyl nitrate (PAN) in suburban and remote areas of western China, Atmos. Environ., 43, 228-237, doi:10.1016/j.atmosenv.2008.09.070, 2009.

Zhang, L., Jacob, D. J., Boersma, K. F., Jaffe, D. A., Olson, J. R., Bowman, K. W., Worden, J. R., Thompson, A. M., Avery, M. A., Cohen, R. C., Dibb, J. E., Flock, F. M., Fuelberg, H. E., Huey, L. G., McMillan, W. W., Singh, H. B., and Weinheimer, A. J.: Transpacific transport of ozone pollution and the effect of recent Asian emission increases on air quality in North America: An integrated analysis using satellite, aircraft, ozonesonde, and surface observations, Atmos. Chem. Phys., 8, 6117-6136, doi:10.5194/acp-8-6117-2008, 2008.

Zhao, B., Wang, S. X., Liu, H., Xu, J. Y., Fu, K., Klimont, Z., Hao, J. M., He, K. B., Cofala, J., and Amann, M.: NOx emissions in China: historical trends and future perspectives, Atmos. Chem. Phys., 13, 9869–9897, doi:10.5194/acp-13-9869-2013, 2013.

Zhu, L., Fischer, E. V., Payne, V. H., Worden, J. R., and Jiang, Z.: TES observations of the interannual variability of PAN over Northern Eurasia and the relationship to springtime fires, Geophys. Res. Lett., 42, 7230-7237, dio:10.1002/2015GL065328, 2015.

Zhu, L., Payne, V. H., Walker, T. W., Worden, J. R., Jiang, Z., Kulawik, S. S., and Fischer, E. V.: PAN in the eastern Pacific free troposphere: A satellite view of the sources, seasonality, interannual variability, and timeline for trend detection, J. Geophys, Res.-Atmos., 122, 3614-3629, doi:10.1002/2016JD025868, 2017.

650 **Tables**

651

652 Table 1. Chemical and meteorological characteristics of the four episodes.

	Episode 1	Episode 2	Episode 3	Episode 4
Type	Transport dominant	Transport dominant	Chemical transformation	Chemical transformation
Event	O_3 export	O_3 export	Haze	Haze
O_3 (ppbv)	60.2 (80.6)	45.6 (62.8)	59.7 (78.9)	61.8 (87.5)
PAN (ppbv)	0.5 (0.9)	0.5 (0.8)	1.2 (2.0)	1.3 (2.4)
$PM_{2.5}$ ($\mu g/m^3$)	34 (62)	23 (36)	50 (76)	77 (156)
SO_2 (ppbv)	4.3 (12.9)	2.0 (4.4)	2.6 (5.4)	4.4 (9.5)
NO_2 (ppbv)	3.7 (7.3)	6.2 (12.1)	6.2 (12.7)	6.1 (9.9)
Wind Speed (m/s)	13.5 (16.0)	9.5 (16.1)	6.6 (10.2)	5.0 (7.7)

653 *Measurements are given for the average with the maximum in the parenthesis.

654 **Figure Captions**

655

656 Figure 1. Temporal variations (against local time) of measured species, including PAN, $PM_{2.5}$,
657 O_3, NO_2, NO, SO_2, and, CO, and meteorological parameters, including relative
658 humidity, temperature, and wind speed in fall 2010. Episodes 1–4, described in the
659 main text, are shaded in blue and yellow.

660 Figure 2. Diurnal variations in the concentrations of O_3, NO_2, PAN, and $PM_{2.5}$, measured at
661 GCO in the fall of 2010 (5 min data of O_3, NO_2, 2 min data of PAN, and 1 h data of
662 $PM_{2.5}$).

663 Figure 3. Comparison of O_3 with the PAN daily maxima. The time when the daily maximum
664 appears is classified as daytime (08–18 h) and nighttime (the rest) based on the
665 time of sunrise and sunset. Numerals indicate the days.

666 Figure 4. The three-day NOAA HYSPLIT backward trajectories of air masses for every one
667 hour observed at GCO during episode 1 (Oct. 31to Nov. 2), episode 2 (Oct. 28–29),
668 episode 3 (Oct. 20–21), and episode 4 (Nov. 4–5). They are colored according to
669 the level of (a) PAN, (b) O_3, (c) NO_2, and (d) $PM_{2.5}$ at GCO at the time of the
670 trajectory initialization. The trajectories north of 50°N are not shown. For these
671 horizontal trajectories, (e) vertical heights are given.

672 Figure 5. Correlations among PAN, $PM_{2.5}$, O_3, and NO_2: (a) O_3 and PAN, (b) NO_2 and PAN,
673 and (c) O_3 and PAN. The lines in (a) and (b) represent the linear regression for each
674 episode.

675 Figure 6. Correlations among PAN, K^+ ion of $PM_{1.0}$, and carbon components of $PM_{2.5}$ for
676 three cases: (a) $PM_{2.5}$ mass and PAN, (b) $PM_{2.5}$ OC and PAN, (d) $PM_{2.5}$ OC and EC,
677 and (d) $PM_{1.0}$ K^+ and PAN. The lines represent the linear regression for each
678 episode.

679 Figure 7. Comparison between the observed and calculated (a) PAN and (b) O_3
680 concentrations by CAM-chem model. Time is given in local time and four episodes
681 are shaded.

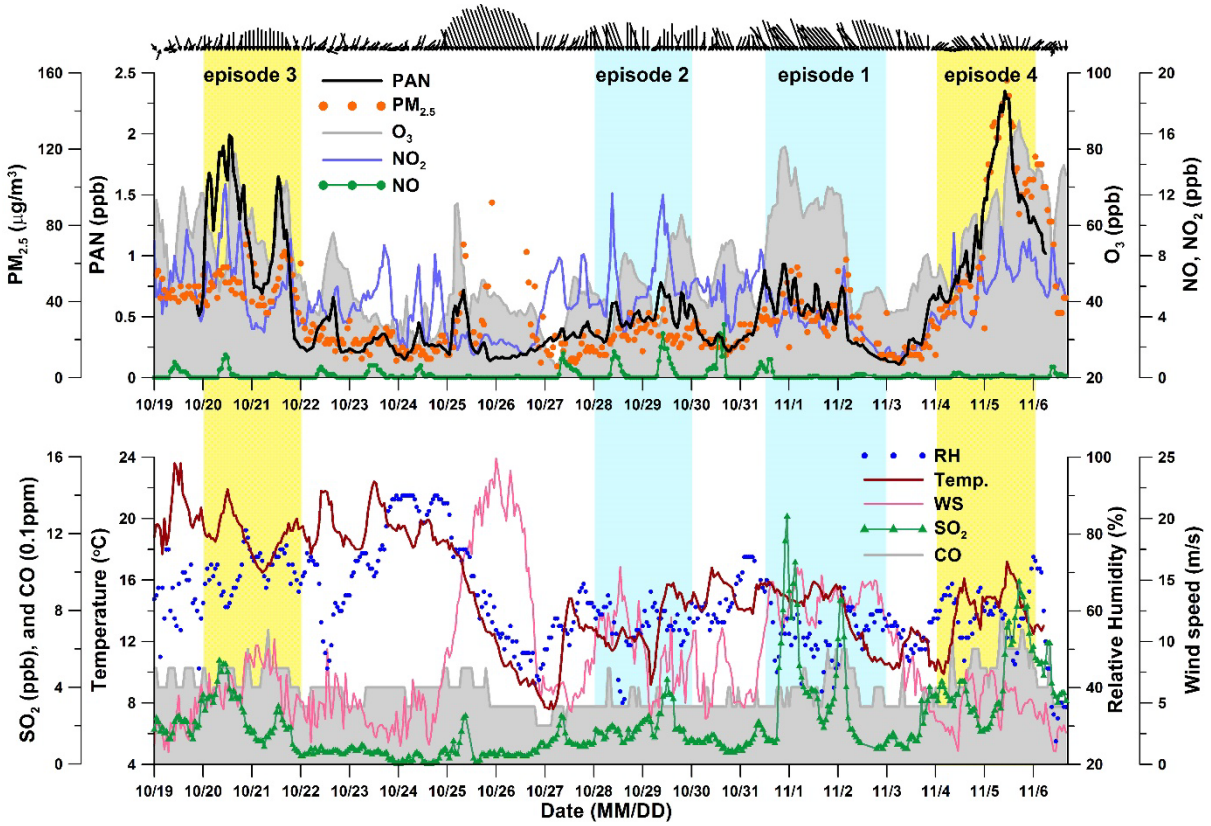

682

683 Figure 1.

684

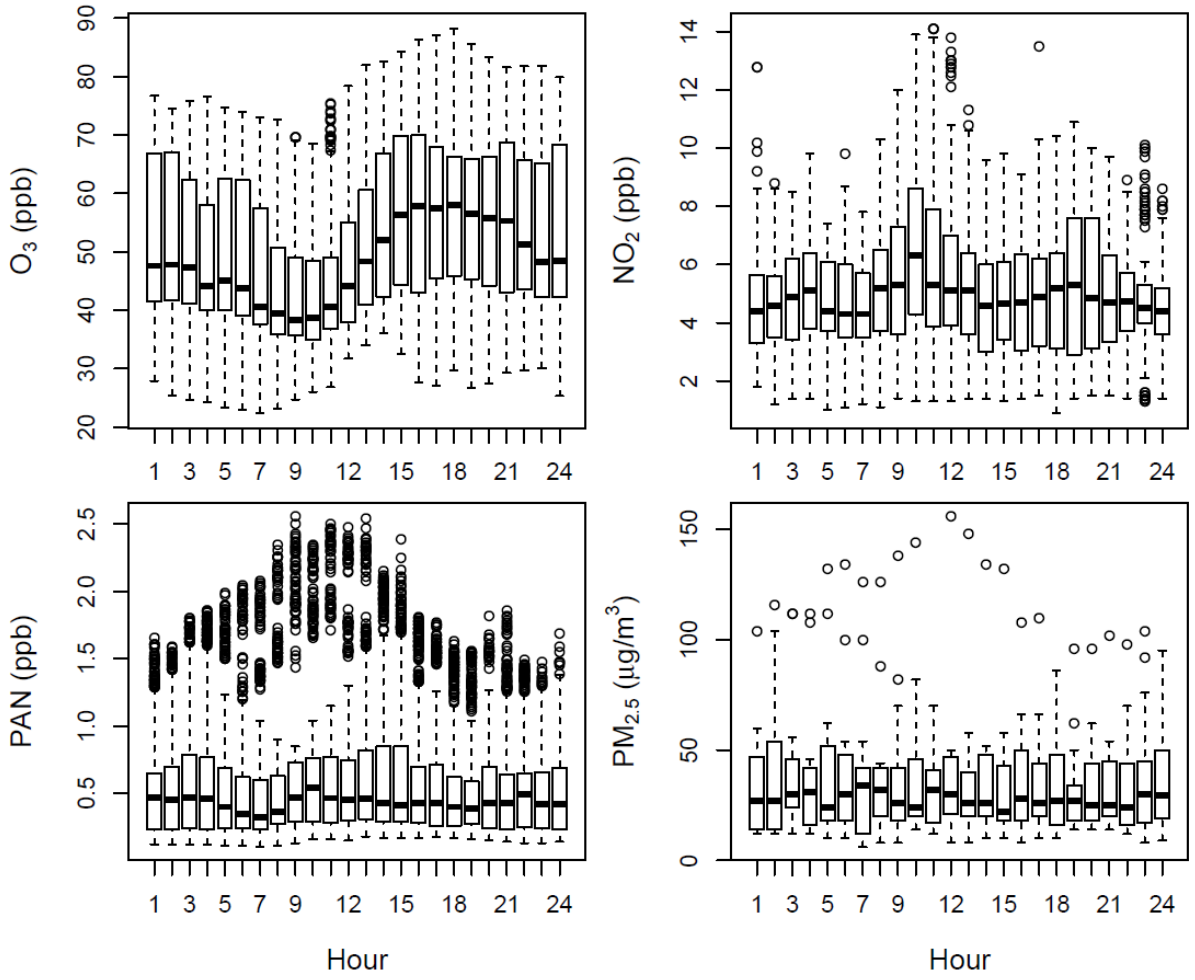

685

686 Figure 2.

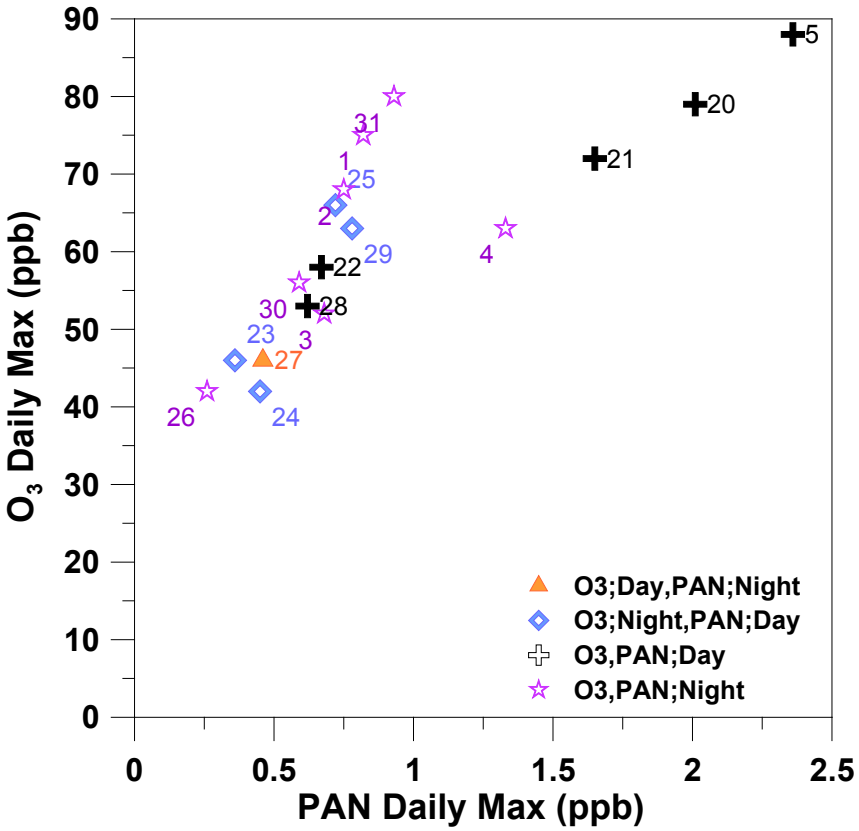

687

688 Figure 3.

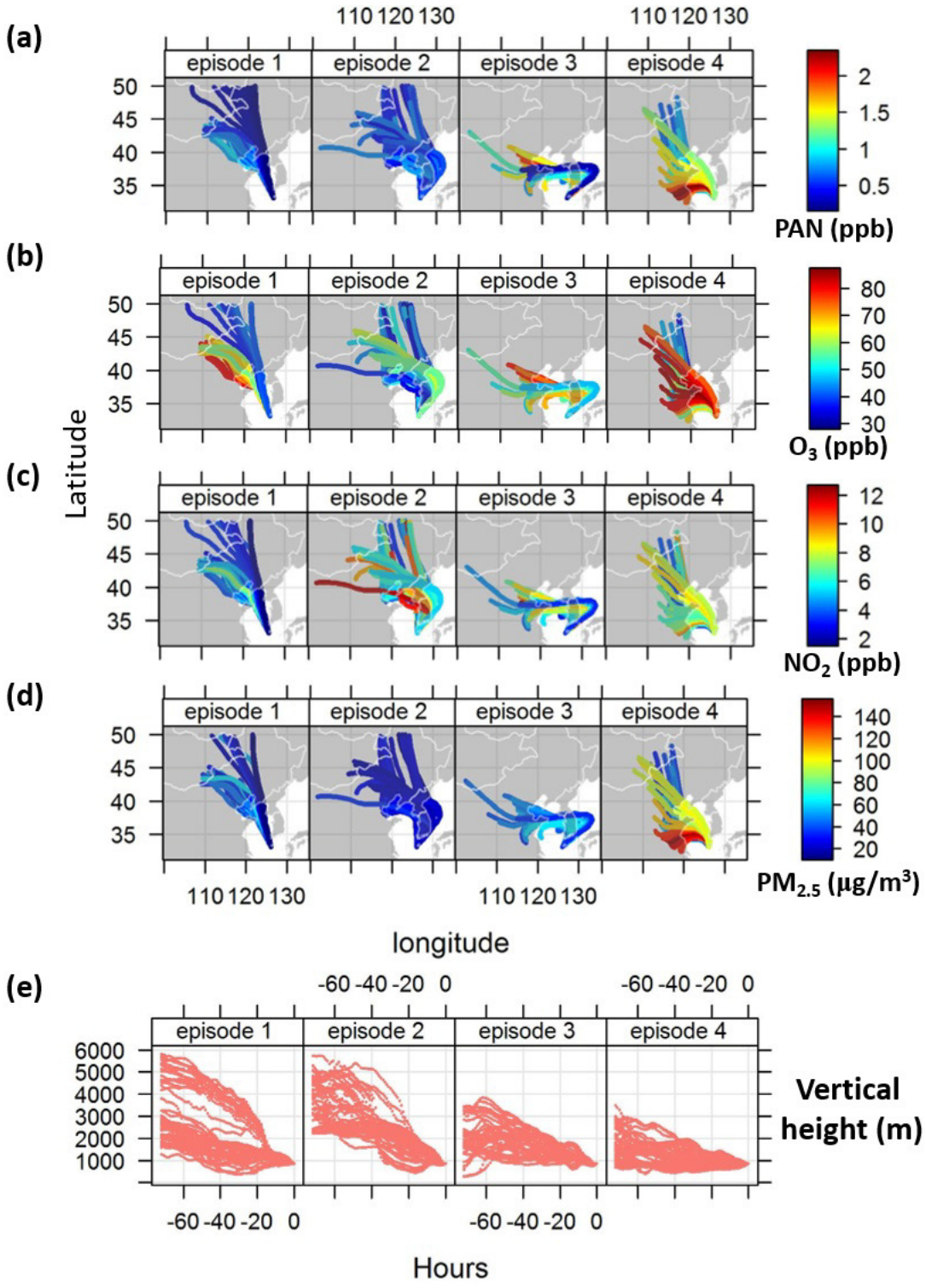

689

690 Figure 4.

691

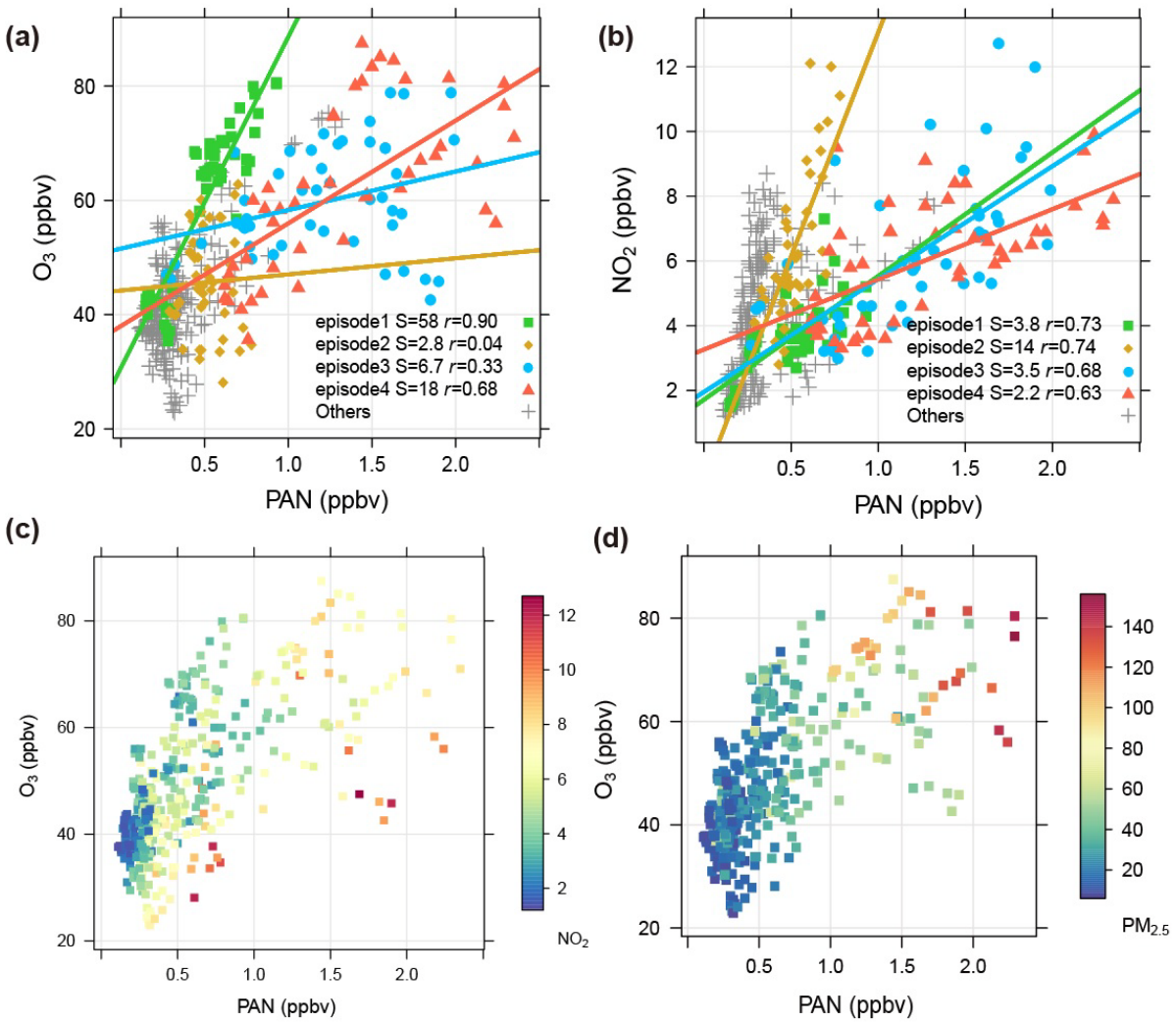

692

693 Figure 5.

694

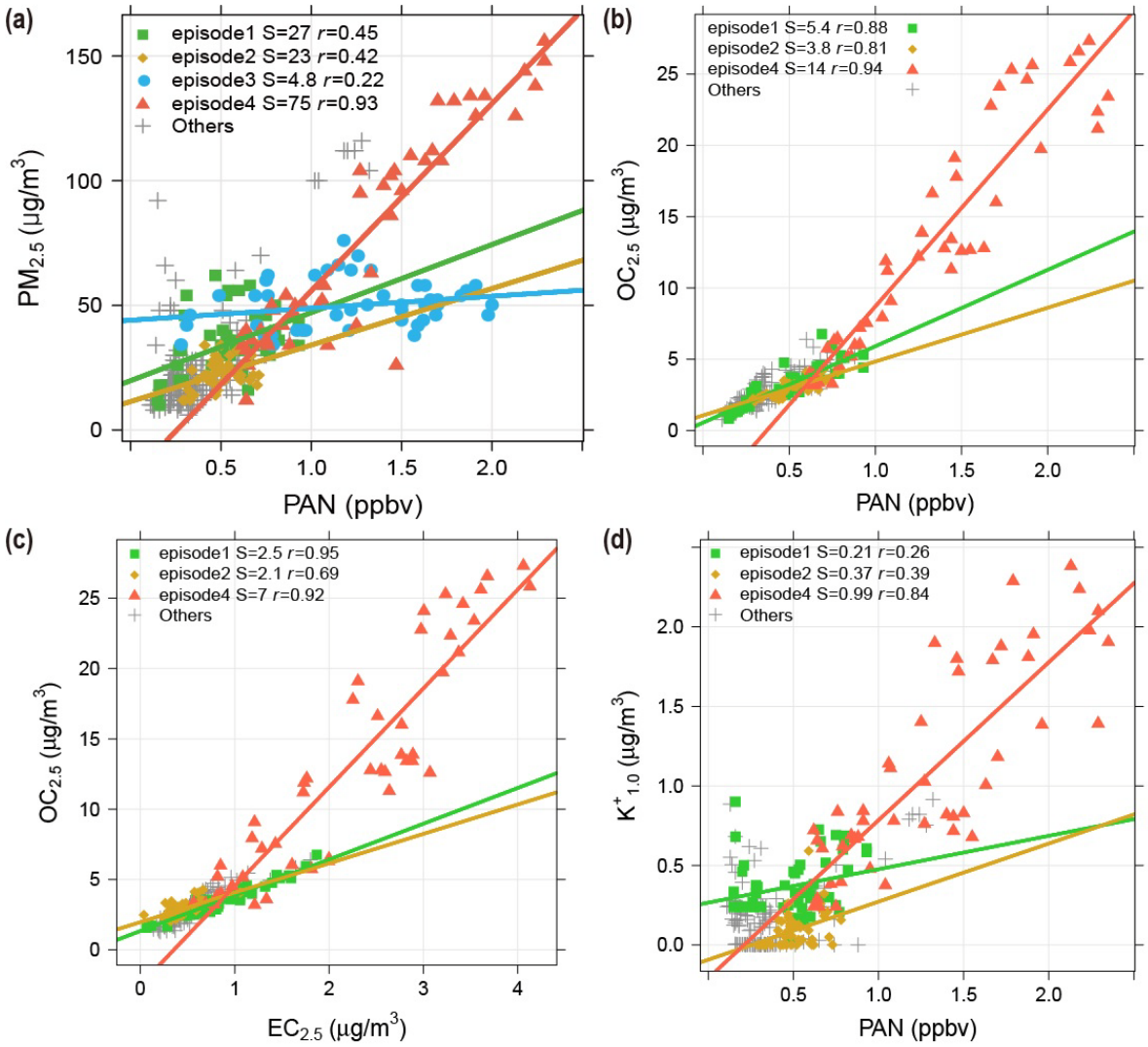

695

696 Figure 6.

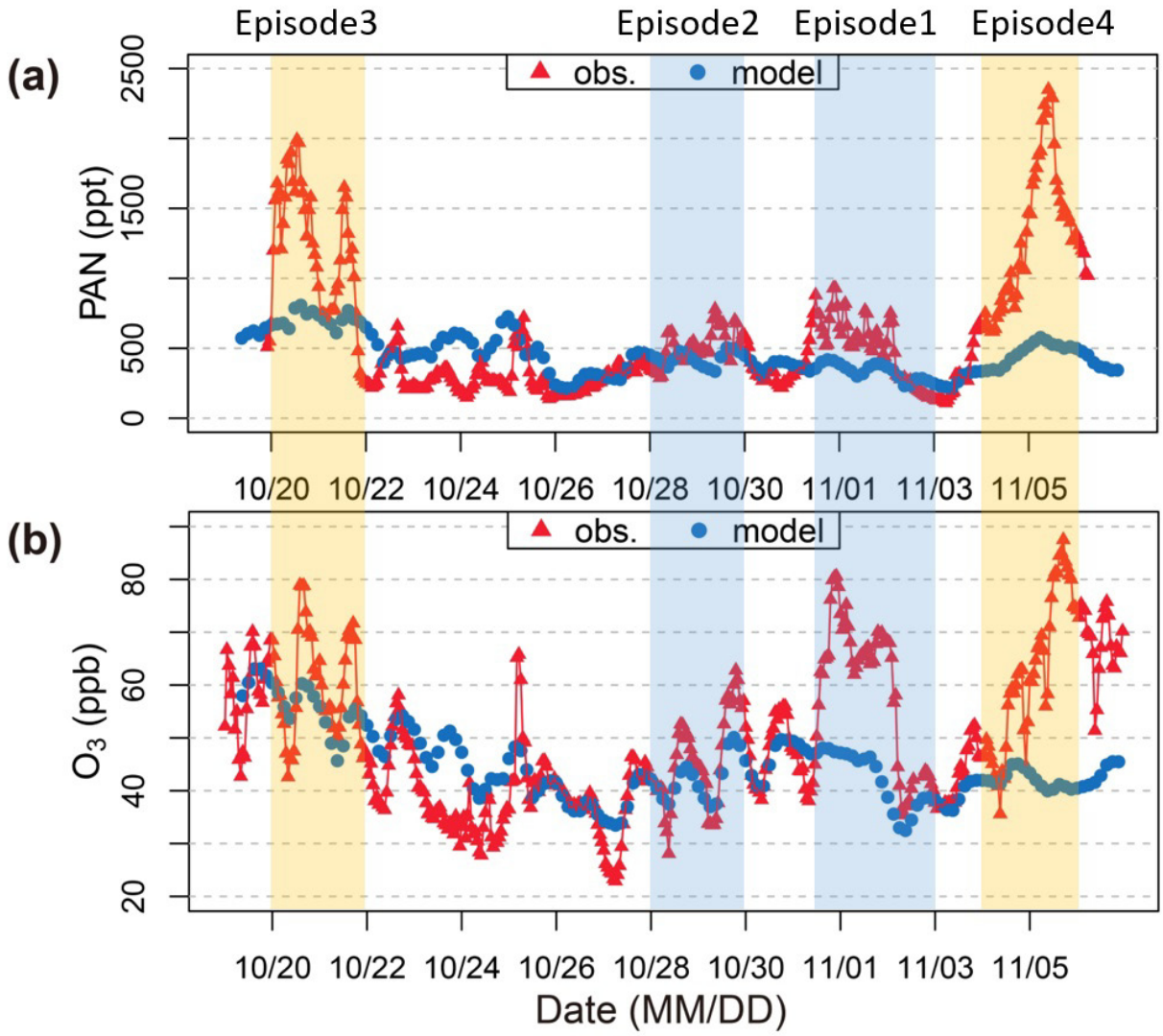

697

698 Figure 7.